High-Strain Sensors Based on ZnO Nanowire/Polystyrene Hybridized Flexible Films

Xu Xiao, Longyan Yuan, Junwen Zhong, Tianpeng Ding, Yu Liu, Zhixiang Cai, Yaoguang Rong, Hongwei Han, Jun Zhou, and Zhong Lin Wang**

Stretchable and transparent electronics that have the ability to conform to and cover deformable and arbitrarily shaped objects are becoming one of the most interesting research fields due to the proliferation of modern society's demand for portable and wearable consumer electronics.[1–3] Approaches to replace rigid substrates by stretchable and flexible ones have been developed to fabricate optoelectronic and electromechanic devices, which have the potential to open promising opportunities in a variety of fields including foldable sensors, roll-up displays, and therapeutics.[4–10]

Buildings, bridges, and other critical infrastructures are sometimes subjected to severe natural disasters, such as hurricanes and earthquakes. To prevent catastrophic failures, it is necessary to monitor the state of these structures in real time using strain sensors.[11] Conventional rigid materials such as ultrathin silicon had been used to fabricate strain sensors, however, the materials exhibit a small tolerable strain, above which the sensors have a risk of failure.[12–14] Strain sensors with ultrahigh flexibility and stretchability will play a key role in personal health monitoring, human-benign devices, highly sensitive robot sensors such as "smart" surgical gloves, and so on.[7,15] Recently, there has been rapid progress on fabricating flexible or stretchable strain sensors based on nanotube and nanowire polymer compositions.[15–19] However, the fabrication of stretchable and sensitive strain sensor with ultrahigh tolerable strain is still a challenge.[15,20]

Here, we introduce a new type of stretchable strain sensor with ultrahigh tolerable strain based on ZnO nanowire (NW)/polystyrene nanofiber (PSNF) hybrid structure on a polydimethylsiloxane (PDMS) film. The novel strain sensor can measure and withstand strain up to ≈50%, with high durability, fast response, and high sensitivity. The device also demonstrated a good performance on small and rapid human-motion measurements. In addition, the device could be driven by solar cells and has potential applications as an outdoor sensor system.

Figure 1 illustrates the schematic depiction of the fabrication of ZnO NW/PSNF hybrid structure. First, PSNFs (Figure S1, Supporting Information) were electrospun on a cured PDMS film (2 cm × 1 cm × 0.1 cm), as shown in Figure 1a, onto which ZnO seeds were "sowed" through immersion of the PSNFs into ZnO naoparticles solution (Figure 1b).[21,22] Then ZnO NWs were grown from the ZnO seeds by a simple hydrothermal process (Figure 1c).[23–25] The scanning electron microscopy (SEM) images of the ZnO NWs grown on PSNFs are shown in Figure 1d,e. It can be seen that ZnO NWs grew on the surface of PS NFs uniformly and formed a ZnO/PS hybrid network structure (Figure 1d). The hybrid film was highly flexible and robust and could bear large deformation without cracking (Figure S3, Supporting Information). Furthermore, ZnO NWs were grown densely around a PSNF axis with the diameter of 50–100 nm and the length of ≈3 μm (inset of Figure 1e), forming a "nanobrush" structure (Figure 1e). X-ray diffraction (XRD) was applied to characterize the crystal structure of ZnO nanowires and is shown in Figure S2 (Supporting Information). All of the diffraction peaks can be indexed to hexagonal wurtzite structure ZnO.

The transmittance of pure PDMS and the ZnO NW/PSNF hybrid structure on PDMS is shown in Figure S4 (Supporting Information). The transmittance of pure PDMS was about 90% from 300 nm to 800 nm. After the formation of ZnO NWs/PSNFs hybrid structure on the surface of PDMS, the hybrid film became semitransparent, which can be seen in the left inset of Figure S4 (Supporting Information). The transmittance of the film was ≈16% at 600 nm, decreasing gradually with the decrease of light wavelength, then reduced to 0 at ≈380 nm due to the band-edge absorption of ZnO.[26]

The study of the electromechanical behavior of the strain sensor was carried out in atmosphere at room temperature. The schematic diagram of the strain sensor is shown in the inset of **Figure 2**a. To make a good contact, Ti (30 nm)/Ag (80 nm) electrodes were deposited on each end of the device through a shadow mask. A PDMS thin layer was used to package the device. The device could be stretched with a strain up to ≈50% (Figure S5, Supporting Information). In comparison, a ZnO thin film and a ZnO nanowire on PDMS film can only tolerate a strain up to ≈6.2% and ≈12%, respectively (Figure S6, Supporting Information). Figure 2a,b show the current–voltage (*I*–*V*) curves and the relative change in resistance of a typical device (with an original resistance of ≈2.2 GΩ) under different strain at a fixed bias of 10 V, respectively. It can be seen that the current decreased gradually and the

X. Xiao, Dr. L. Y. Yuan, J. W. Zhong, T. P. Ding, Y. Liu, Dr. Z. X. Cai, Y. G. Rong, Prof. H. W. Han, Prof. J. Zhou, Prof. Z. L. Wang
Wuhan National Laboratory for Optoelectronics (WNLO)
College of Optoelectronic Science and Engineering
Huazhong University of Science and Technology (HUST)
Wuhan, 430074, P. R. China
E-mail: jun.zhou@mail.hust.edu.cn
Prof. Z. L. Wang
School of Materials Science and Engineering
Georgia Institute of Technology
Atlanta, Georgia 30332-0245, USA
E-mail: zhong.wang@mse.gatech.edu

DOI: 10.1002/adma.201103406

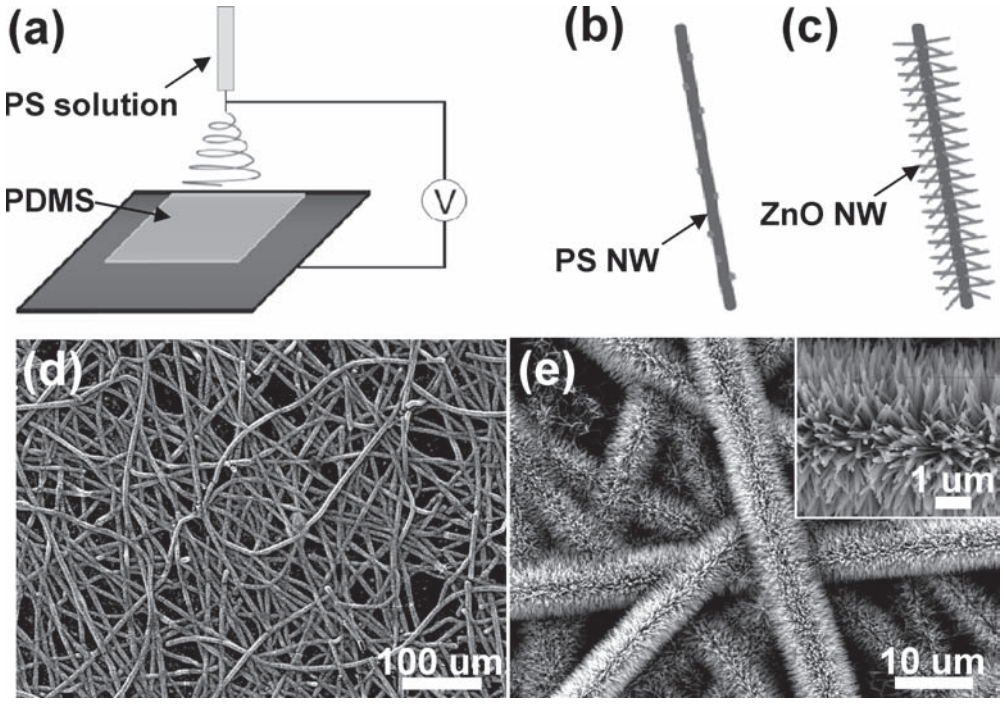

Figure 1. a–c) Schematic depiction of the fabrication of ZnO NWs/PSNFs hybrid structure. d,e) SEM images of ZnO NW/PSNF hybrid structure. The inset in (e) shows the high-resolution SEM image of the ZnO NWs.

relative change in resistance increased monotonously when the device was stretched under strain from 0% to 50%. The ultrahigh tolerable strain of the sensor can be attributed to the highly stretchable PSNFs networks since some curved fibers in the PSNFs networks could be straightened under strain thus release a part of the strain applied to the device (Figure S1, Supporting Information). It is possible that the current flows through the ZnO NWs and contact points among them. These contact points would decrease when the device was elongated, and the number of the electrical passways would be reduced accordingly, resulting in an increase in the electrical resistance of the device. In addition, when the fabricated strain sensor was stretched, the cross-section area of the device was reduced, and the device's length increased, both of which led to the resistance increase for the device.

The relative change in resistance under strain shows a linear behavior. The slope reflects the gauge factor that is defined as $(dR/R)/(dL/L)$, where R and L are the resistance and length of the device, respectively. The gauge factors were calculated to be ≈116 for the device. This value is lower than the gauge factors (≈1000–1500) of a single nanotube/nanowire based nanosensor;[27,28] comparable with the gauge factor (≈200) of state-of-the-art doped Si strain sensor; and much higher than the gauge factor (≈1–5) of conventional metal gauges, the gauge factor (≈20) of 50 wt% carbon black/polymer composites,[29] and the gauge factor (≈0.06–0.82) of carbon nanotube/polymer composites.[15]

In order to probe the response and recovery properties of the strain sensor, the electromechnical properties of the strain sensor were investigated in detail. The static state electromechanical properties of the strain sensor measured by monitoring the current at different strain state at a fixed voltage of +10 V. We checked the current flow through the device by stretching the device step by step under 0%, 1.5%, 3%, 4%, and 8% strain (each step was held for 15 s) and then released gradually from 8% to 4%, 3%, 1.5%, and 0%, as illustrated in Figure 2c. It can be seen that the current switched rapidly at every turning point, the current remained identical under the same strain, and no remarkable current change was observed at a certain strain state. The device preserved the superb response and recovery properties even under an ultrahigh strain of ≈30% (Figure 2d), which indicates attractive perspective in applications such as precision measurements.

It is now widely accepted that environentally benign devices will be very important for future applications in daily life for health monitoring and entertainment purposes.[30,31] We tested the electromechanical sensing of the fabricated sensor on the human body to demonstrate the potential uses in wearable electronics. An as-fabricated strain sensor was fixed onto an index finger. We checked the currents flow through the device (at a fixed voltage of +10 V) at four different bending and release motions of the finger, which are labeled as state I, II, III, and IV in the upper insets in **Figure 3**. In each bending–unbending motion, the finger bent to the same angle in every cycle, held for 10 s, and then released. It can be observed that the sensor responsed to the motion of the finger rapidly and the current recovered to the original value at every bending–release motion (Figure 3). More importantly, the current remained almost stable in each bending state, considering to the trembling of the finger. Furthermore, the strain sensor fixed on a tile showed a

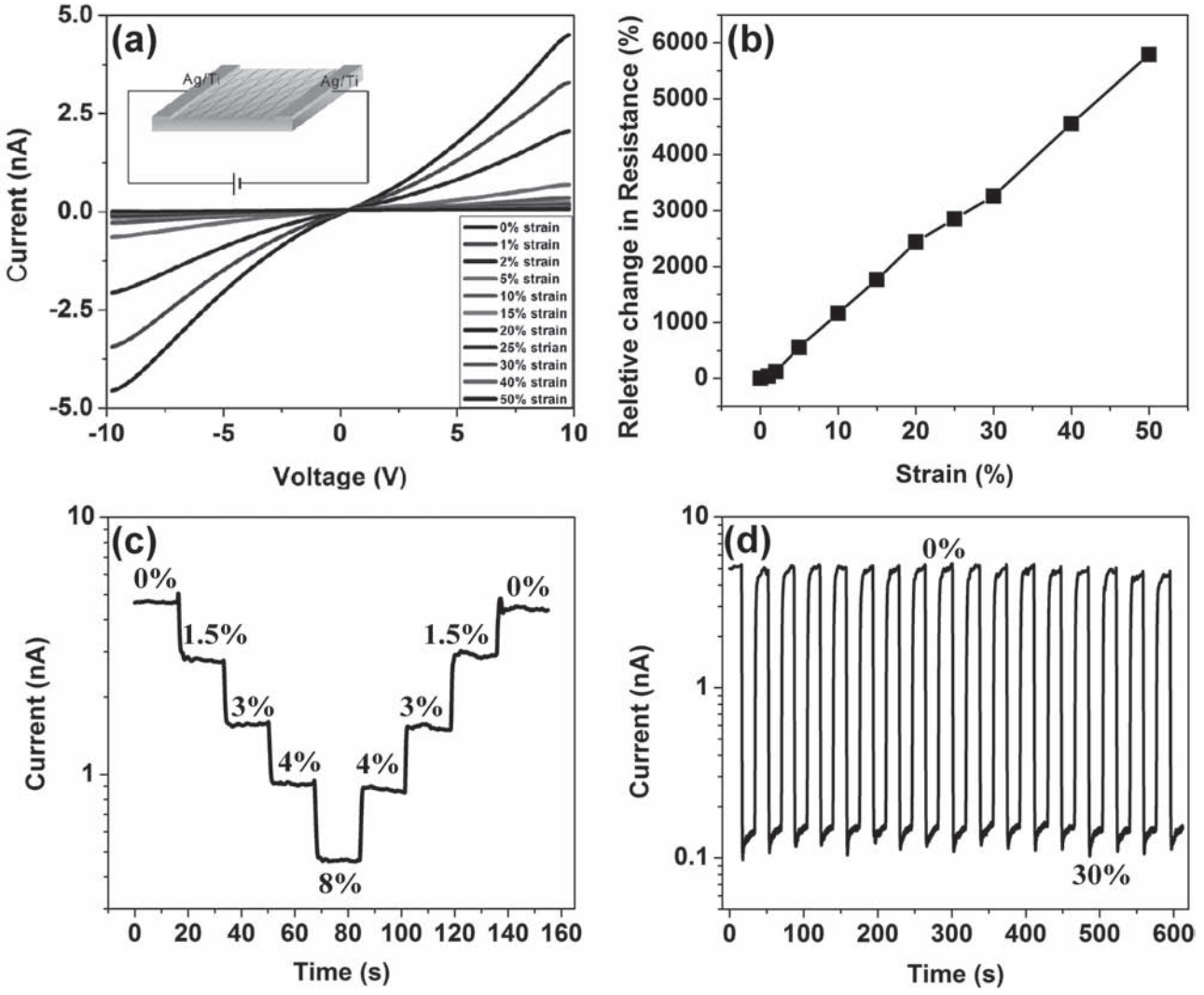

Figure 2. Electromechanical behaviors of the strain sensor. a,b) *I–V* curves and the relative change in resistance of the device under different strain. The inset of (a) is the schematic diagram of the strain sensor. c,d) Current response of the strain sensor device at different static strain state under a fixed bias of 10 V.

sharp and rapid response (Figure S7, Supporting Information) when the tile was broken by a hammer. This result indicates that our strain sensors have the potential application for the prevention of catastrophic failure.

Finally, we integrated the strain sensor with solar cells, through which the sensor may be operated outdoors. The inset of Figure S8 (Supporting Information)shows a photograph of the solar cell, which is composed of five series-connected monolithic all-solid-state dye-sensitized solar cells.[32] Figure S8 (Supporting Information) shows the current density–voltage curve of the series connected solar cells with an open-circuit voltage of ≈3.7 V under 1.5 AM sun illumination. The solar cell was used to power the sensor device (with an original resistance of ≈9 GΩ) (Figure S9, Supporting Inforamtion), which was cyclically stretched and released by a resonator at a frequency of 2 Hz (Figure S10, Supporting Information). The current response of the sensor with time was shown in **Figure 4**. Remarkably, the current reached almost the same value in each cycle of straining and fully recovered to the state without strain, indicating that the sensor had high reproducibility and good stability. The derived response time of the strain sensor was about 140 ms without considering response time of the measurement system. This demonstration implies that the device has the potential for application in the future self-powered outdoor nanosensor system with high reliability.

In summary, a novel strain sensor prototype based on a ZnO NW/PSNF hybrid structure has been demonstrated. The device can withstand strain up to 50%, with high durability, fast response, and high gauge factors. With flexibility and stretchability, we believe that the device will have potential applications in nanosensor systems for precision measurements, human skins, person health monitoring, and remote-controlled smart robot surgical hands.

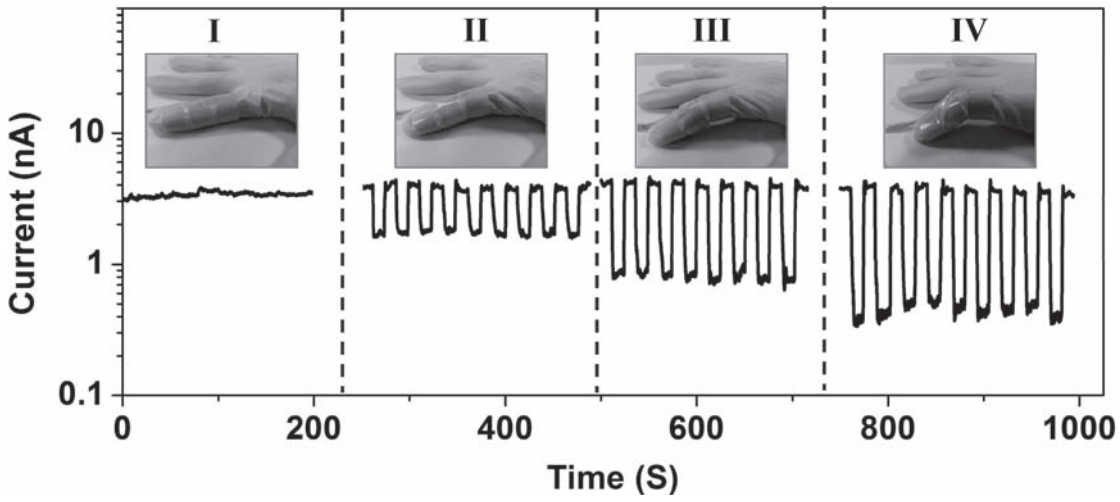

Figure 3. The curent–time (*I–T*) response curve of the strain sensor device that was fixed on an index finger at four different bending and release finger motions under a fixed bias of 10 V. The upper insets labeled as I, II, III, and IV demonstrate the four finger motion states.

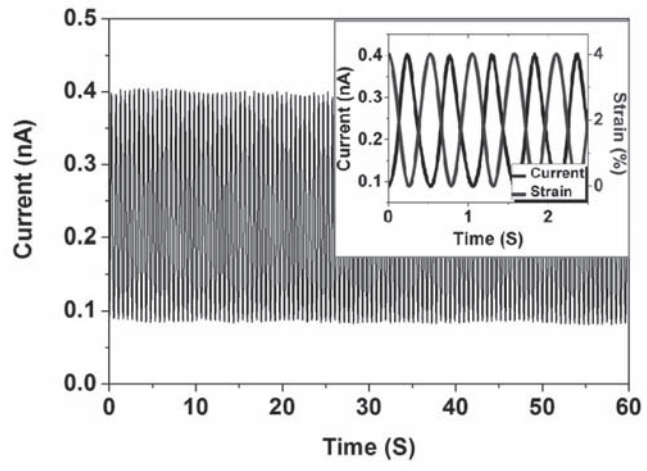

Figure 4. Current response of the sensor device that was powered by solar cells. The device was driven by a resonator with cyclical stretching and releasing at a frequency of 2 Hz. The inset shows the current response of the sensor device and the corresponding strain with time in 2.5 s.

Experimental Section

Method for Electrospinning PSNFs on the PDMS Film: 0.7 g polystyrene (PS) was dissolved in a mixture of 1.5 mL dimethylformamide (DMF) and 1.5 mL toluene. Before the solution was transferred into a 2.5 mL syringe for electrospinning, the mixture was stirred at a speed of 300 rps (rotations per s) for ≈3 h. During the electrospinning process, a direct current voltage of 20 kV was applied to the syringe needle and collector, and a feed rate of 0.1875 μL s^{-1} was used. The distance between the needle tip and the collector was 20 cm. A small piece of PDMS film (prepared by mixing the PDMS base and curing agent with a 10:1 w/w ratio and cured at 60 °C for 1 h) on the tinfoil as the collector. The electrospinning process lasted ≈3 min.

Growth of ZnO NWs on PSNFs: The ZnO NWs were grown on PSNFs through immobilization of ZnO seeds onto PS NFs, followed by a hydrothermal process. First, zinc acetate dihydrate (0.01 M) and KOH (0.03 M) were used for the preparation of the ZnO seed solution. Zinc acetate dihydrate dissolved in methanol was stirred vigorously at ≈60 °C with a solution of KOH in methanol added dropwise at 60 °C, then stirred the reaction mixture at 60 °C for 2 h. Subsequently, the substrate was immersed in the ZnO seed solution for 50–60 s. 16 mM equimolar solutions of hexamethylenetetramine and zinc nitrate and ≈3 to 4.5 mL of ammonia (pH ≈ 10.9) were used for further growth at 95 °C for ≈12 to 14 h. After the reaction, the products were washed softly with deionized water and dried in 60 °C oven.

Properties of Strain Sensor Measurements: The original *I–V* measurements of the device under different strain were carried out on a homemade probe station. After electrodes were deposited on the each end of device, PDMS was used to package the device. The device was placed and fixed on two separate mechanical stages with a fine moving step of 2 μm. A synthesized function generator (Model DS345, Stanford Research Systems, USA) and a low-noise current preamplifier (Model SR570, Stanford Research Systems, USA) were used to measure the *I–V* curves. The current–time (*I–T*) response was studied by using a swept signal generator (YE 1311-D, Sinocera, China) and a strong resonator (JZK, Sinocera, China). One end of the device was fixed on the stage and the other end was fixed on the resonator for stretching. The human-motion sensing behavior was measured by the function generator and preamplifier. The *I–V* characteristics of solar cell were measured by using a Keithley 2400 source meter under 1.5 AM sun illumination (91160, Newport).

Transmittance Measurements: The transmittances of PDMS and ZnO/PS hybrid structure were measured using a spectrophotometer UV-2550 (Shimadzu, Japan).

Supporting Information

Supporting Information is available from the Wiley Online Library or from the author.

Acknowledgements

X.X. and L.Y.Y. contribted equally to this work. This work was financially supported by the National Natural Science Foundation of China (51002056), a Foundation for the Author of National Excellent Doctroal Dissertation of P. R. China (201035), the Program for New Century

Excellent Talents in University (NCET-10-0397), and China Postdoctoral Science Foundation (20100480892). The authors are also thankful for the support from Huazhong University (01-24-182021, 01-24-187051). The authors thank the Analysis and Testing Center of Huazhong University of Science and Technology for support.

Received: September 4, 2011
Published online: October 17, 2011

[1] T. Sekitani, Y. Noguchi, K. Hata, T. Fukushima, T. Aida, T. Someya, *Science* **2008**, *321*, 1468.
[2] H. C. Ko, M. P. Stoykovich, J. Song, V. Malyarchuk, W. M. Choi, C. J. Yu, J. B. Geddes, J. Xiao, S. Wang, Y. Huang, J. A. Rogers, *Nature* **2008**, *454*, 748.
[3] K. Takei, T. Takahashi, J. C. Ho, H. Ko, A. G. Gillies, P. W. Leu, R. S. Fearing, A. Javey, *Nat. Mater.* **2010**, *9*, 821.
[4] S. R. Forrest, *Nature* **2004**, *428*, 911.
[5] D. Y. Khang, H. Jiang, Y. Huang, J. A. Rogers, *Science* **2006**, *311*, 208.
[6] H. E. A. Huitema, G. H. Gelinck, J. B. P. H. van der Putten, K. E. Kuijk, C. M. Hart, E. Cantatore, P. T. Herwig, A. J. J. M. van Breemen, D. M. de Leeuw, *Nature* **2001**, *414*, 599.
[7] D. H. Kim, J. H. Ahn, W. M. Choi, H. S. Kim, T. H. Kim, J. Song, Y. Y. Huang, Z. Liu, C. Lu, J. A. Rogers, *Science* **2008**, *320*, 507.
[8] X. H. Zhang, L. Gong, K. Liu, Y. Z. Cao, X. Xiao, W. M. Sun, X. J. Hu, Y. H. Gao, J. Chen, J. Zhou, Z. L. Wang, *Adv. Mater.* **2010**, *22*, 5292.
[9] L. Y. Yuan, Y. T. Tao, J. Chen, J. J. Dai, T. Song, M. Y. Ruan, Z. W. Ma, L. Gong, K. Liu, X. H. Zhang, X. J. Hu, J. Zhou, Z. L. Wang, *Adv. Funct. Mater.* **2011**, *21*, 2150.
[10] L. Y. Yuan, J. J. Dai, X. H. Fan, T. Song, Y. T. Tao, K. Wang, Z. Xu, J. Zhang, X. D. Bai, P. X. Lu, J. Chen, J. Zhou, Z. L. Wang, *ACS Nano* **2011**, *5*, 4007.
[11] H. Gullapalli, V. S. M. Vemuru, A. Kumar, A. Botello-Mendez, R. Vajtai, M. Terrones, S. Nagarajaiah, P. M. Ajayan, *Small* **2010**, *6*, 1641.
[12] C. S. Smith, *Phys. Rev.* **1954**, *94*, 42.
[13] R. He, P. D. Yang, *Nat. Nanotechnol.* **2011**, *1*, 42.
[14] G. Park, T. Rosing, M. D. Todd, C. R. Farrar, W. Hodgkiss, *ASCE J. Infrastruct. Syst.* **2008**, *14*, 64.
[15] T. Yamada, Y. Hayamizu, Y. Yamamoto, Y. Yomogida, A. Izadi-Najafabadi, D. N. Futaba, K. Hata, *Nat. Nanotechnol.* **2011**, *6*, 296.
[16] H. Maune, M. Bockrath, *Appl. Phys. Lett.* **2006**, *89*, 173131.
[17] K. J. Loh, J. Kim, J. P. Lynch, N. W. S. Kam, N. A. Kotov, *Smart Mater. Struct.* **2007**, *16*, 429.
[18] M. Park, H. Kim, J. P. Youngblood, *Nanotechnology* **2008**, *19*, 055705.
[19] C. L. Chen, E. Lopez, Y. J. Jung, S. Müftü, S. Selvarasah, M. R. Dokmeci, *Appl. Phys. Lett.* **2008**, *93*, 093109.
[20] K. Liu, Y. H. Sun, P. Liu, X. Y. Lin, S. S. Fan, K. L. Jiang, *Adv. Funct. Mater.* **2011**, *21*, 2721.
[21] C. Pacholski, A. Kornowski, H. Weller, *Angew. Chem. Int. Ed.* **2002**, *41*, 1188.
[22] H. Ko, Z. Zhang, K. Takei, A. Javey, *Nanotechnology* **2010**, *21*, 295305.
[23] L. Vayssieres, *Adv. Mater.* **2003**, *15*, 464.
[24] S. Xu, Y. G. Wei, M. Kirkham, J. Liu, W. J. Mai, D. Davidovic, R. L. Snyder, Z. L. Wang, *J. Am. Chem. Soc.* **2008**, *130*, 14958.
[25] S. Xu, Y. Shen, Y. Ding, Z. L. Wang, *Adv. Funct. Mater.* **2010**, *20*, 1493.
[26] Y. K. Tseng, C. J. Huang, H. M. Cheng, I. N. Lin, K. S. Liu, I. C. Chen, *Adv. Funct. Mater.* **2003**, *13*, 811.
[27] J. Zhou, Y. Gu, P. Fei, W. Mai, Y. Gao, R. Yang, G. Bao, Z. L. Wang, *Nano Lett.* **2008**, *8*, 3035.
[28] J. Cao, Q. Wang, H. Dai, *Phys. Rev. Lett.* **2003**, *90*, 157601.
[29] C. Mattmann, F. Clemens, G. Troster, *Sensors* **2008**, *8*, 3719.
[30] T. Someya, T. Sekitani, S. Iba, Y. Kato, H. Kawaguchi, T. Sakurai, *Proc. Natl. Acad. Sci. USA* **2004**, *101*, 9966.
[31] K. Nomura, H. Ohta, A. Takagi, T. Kamiya, M. Hirano, H. Hosono, *Nature* **2004**, *432*, 488.
[32] H. Wang, G. H. Liu, X. Li, P. Xiang, Z. L. Ku, Y. G. Rong, M. Xu, L. F. Liu, M. Hu, Y. Yang, H. W. Han, *Energy Environ. Sci.* **2011**, *4*, 2025.